NATIONAL ENERGY TECHNOLOGY LABORATORY

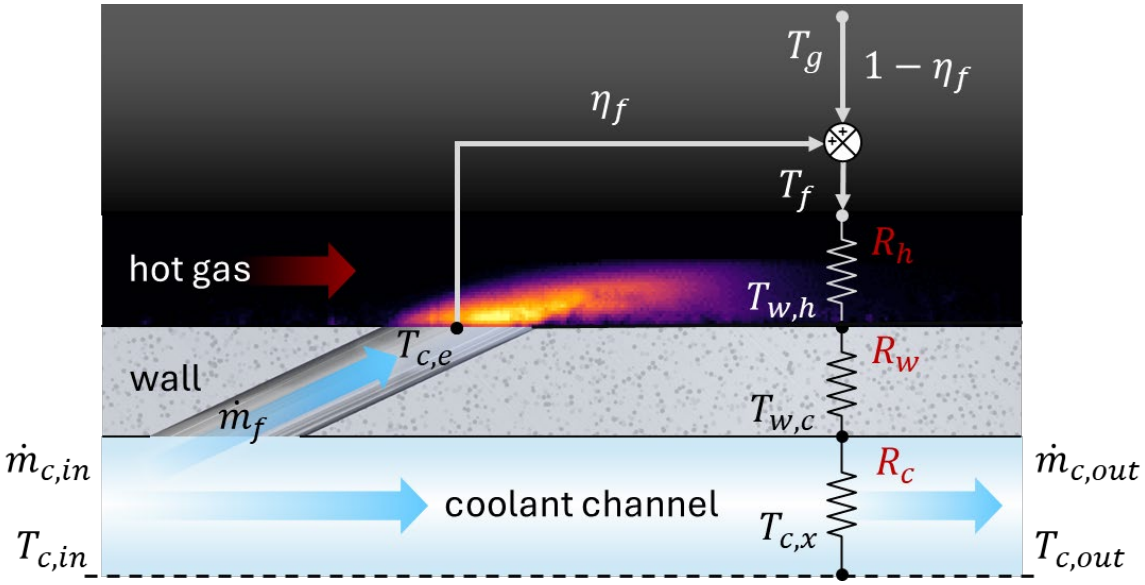

Simple Heat Transfer Model for Film Cooling Applications

30 January 2025

U.S. DEPARTMENT of ENERGY

Office of Fossil Energy and Carbon Management

DOE/NETL-2025/4912

Disclaimer

This project was funded by the United States Department of Energy, National Energy Technology Laboratory, in part, through a site support contract.

Cover Illustration: Simplified thermal resistance network model for film cooling

Suggested Citation: Straub, Douglas; Tulgestke, Andrew; Searle, Matthew, and Robey, Edward. *Simple Heat Transfer Model for Film Cooling Applications*; DOE/NETL-2025/4912; NETL Technical Report; U.S. Department of Energy, National Energy Technology Laboratory: Morgantown, WV, 2025.

An electronic version of this report can be found at:

https://netl.doe.gov/energy-analysis/search

Simple Heat Transfer Model for Film Cooling Applications

Douglas Straub[1]; Andrew Tulgestke[1,2]; Matthew Searle[1], and Edward Robey[1,2]

[1] National Energy Technology Laboratory, 3610 Collins Ferry Road, Morgantown, WV 26505, USA

[2] NETL Support Contractor, 3610 Collins Ferry Road, Morgantown, WV 26505, USA

DOE/NETL-2025/4912

30 January 2025

NETL Contacts:

Douglas Straub, Principal Investigator

Pete Strakey, Technical Portfolio Lead

Bryan Morreale, Associate Laboratory Director for Research & Innovation, Research & Innovation Center

This page intentionally left blank.

Table of Contents

List of Figures

List of Tables

Acronyms, Abbreviations, and Symbols

Term	Description
c_p	Specific heat (J/kg K)
k	Thermal conductivity (W/m K)
L	Dimension (m)
$\dot{m}$	Mass flow rate (kg/s)
R	Thermal resistance (K/W)
R''	Specific thermal resistance (m^2 K/W)
S	Surface area for heat transfer (m^2)
t	Wall thickness parallel to direction of heat flow (m)
T	Temperature (K)
U	Overall equivalent heat transfer coefficient (W/m^2K)
W^+	Heat load parameter, $W^+ = \frac{\dot{m}_c c_p}{US_h}$
x	Coordinate parallel to coolant flow direction (m)
z	Coordinate perpendicular to coolant flow direction, and parallel to hot gas flow direction (m)
Greek	
ϕ	Overall cooling effectiveness, $\phi = \frac{T_g - T_w}{T_g - T_{c,in}}$
η_f	Film effectiveness, $\eta_f = \frac{T_g - T_f}{T_g - T_{c,e}}$
χ	Coolant warming factor, $\chi = \frac{T_{c,x} - T_{c,in}}{T_{c,out} - T_{c,in}}$
Subscripts	
c	Cold side
e	Exit of film cooling hole
f	Film
g	Hot gas, or freestream
h	Hot side
in	Coolant channel inlet
out	Coolant channel outlet
TBC	Thermal barrier coating
w	Wall

Acknowledgments

This work was performed in support of the National Energy Technology Laboratory's (NETL) ongoing research under the Hydrogen with Carbon Management Program by NETL's Research and Innovation Center. The authors wish to acknowledge Nate Weiland, John Crane, and Bob Schrecengost for programmatic guidance, direction, and support.

The authors also wish to acknowledge the efforts of Edward Robey for his creativity and diligent efforts to develop the early versions of this model.

Credit

Douglas Straub: conceptual application of model, writing original draft, data analysis, Andrew Tulgestke and Matthew Searle: conceptualization, writing original draft, Edward Robey: Early model development and conceptualization.

EXECUTIVE SUMMARY

This technical report describes the development of a simple engineering model for film cooling. This model is used to relate local wall temperature variations to local heat transfer coefficients and film effectiveness in a way that has not been published previously. The scope of this report includes the derivation of regression model equations *with* and *without* film cooling. The model equation *without* film cooling can be used to estimate local heat transfer coefficients using surface temperatures measured from infrared thermography. The model equation *with* film cooling can be used to estimate film cooling effectiveness, η_f, and heat transfer augmentation, h_f/h_0, for the film cooling jet(s). The model regression equations differ slightly from the expressions derived from the model. For example, experimental data are used to estimate which terms in the derived relations are significant. These and other details are discussed in this report.

This report complements another publication in which the regression model equations developed in this report have been used to predict local surface temperatures with a mean absolute error of less one percent of the average surface temperature. This agreement is significantly better than previous film cooling models, and future effort could enhance this model and improve gas turbine performance.

1. INTRODUCTION

In the pursuit of more efficient gas turbine technologies, cooling hot gas components is a critical technology. Film cooling is subset of the cooling technologies used in today's most advanced gas turbine engines. Film cooling injects a layer of relatively cold air between the hot gas stream and the surface. Although the underlying physics of film cooling has been studied for decades, technical challenges still exist.[1,2,3]

One of the remaining challenges is predicting cooling performance in engine applications. This topic has been an area of significant research for decades. In 1985, Forth[4] provided a thorough review of early analytical heat transfer models (i.e., Eriksen et al.[5] and Holland and Thake[6]). The film cooling model proposed by Eriksen et al.[5] incorporated energy source terms and required local experimental data to fit the height of the source term and to estimate the effective turbulent diffusivity. This analytical model did not include cooling performance parameters such as film effectiveness and heat transfer augmentation. Similarly, the models proposed by Holland and Thake[6] did not originally include film cooling effects. However, subsequent work by Young and Wilcox[7] and Torbidoni and Horlock[8] incorporated film cooling effectiveness to describe a new method of calculating coolant requirements for cycle performance analysis. Downs and Landis[9] incorporated thermal barrier coating protection terms. The current state-of-the-art expression that relates overall cooling effectiveness, or normalized wall temperature, to film cooling performance is shown in Equation 1.

In Equation 1, the normalized metal temperature, or overall cooling effectiveness, ϕ, is a function of three non-dimensional cooling parameters. The three cooling parameters include the following: 1) the internal cooling efficiency, η_{th}, 2) the film effectiveness, η_f, and 3) the non-dimensional coolant mass flow rate, W^+. This relationship assumes the wall temperature is constant, at least in the spanwise direction. Although the constant spanwise wall temperature assumption may be a reasonable for cycle performance models, this assumption may not be appropriate for predicting spanwise surface temperature variations that can affect component life and reliability. Furthermore, the internal cooling efficiency is very difficult to quantify.[10] Finally, Equation 1 neglects heat transfer augmentation effects due to the cooling jets and treats film effectiveness, η_f, and internal cooling efficiency, η_{th}, as parameters that are independent of coolant mass flow rate.

$$\phi = \frac{\eta_f - \eta_f \eta_{th} + \eta_{th} W^+}{1 - \eta_f \eta_{th} + \eta_{th} W^+} \tag{1}$$

$$\phi = \frac{T_g - T_{w,h}}{T_g - T_{c,in}} \tag{2}$$

$$\eta_f = \frac{T_g - T_f}{T_g - T_{c,e}} \tag{3}$$

$$\eta_{th} = \frac{T_{c,out} - T_{c,in}}{T_{w,h} - T_{c,in}} \tag{4}$$

$$W^+ = \frac{\dot{m}_c c_p}{U S_h} \tag{5}$$

$$U = \frac{1}{\left[\frac{1}{h_g A_h} + \frac{t_{TBC}}{k_{TBC} A_h} + \frac{t_w}{k_w A_w} + \frac{1}{h_c A_c}\right]} \tag{6}$$

In a different approach, Albert et al.[11] reported both the film effectiveness and the overall effectiveness (normalized wall temperature) near the leading edge of a film cooled vane. In this study, the importance of heat conduction through the wall was recognized and discussed. In a subsequent study, Albert and Bogard[12] proposed a relationship between overall cooling effectiveness, ϕ_f, and adiabatic film effectiveness as shown in Equation 7. Although Equation 7 is based on an overall thermal resistance model, it does not include a heat transfer augmentation term (i.e, h_f/h_0). Furthermore, other assumptions were made in this expression that may not be valid for non-adiabatic wall boundary conditions (i.e., $T_{c,e} \cong T_{c,in}$). Since significant differences between the model and the experiment were observed by Albert and Bogard[12], a warming factor, χ, was incorporated by subsequent researchers[13,14] as shown in Equation 8. Even when the warming factor was included, the model consistently overpredicted the overall cooling effectiveness measured in a Biot Number matched conjugate heat transfer test[13,14].

$$\phi_f = \frac{1 - \eta_f}{1 + \frac{h_f t_w}{k_w} + \frac{h_f}{h_c}} + \eta_f \tag{7}$$

$$\phi_f = \frac{1 - \chi\eta_f}{1 + \frac{h_f t_w}{k_w} + \frac{h_f}{h_c}} + \chi\eta_f \tag{8}$$

The key distinctions between the model described in this report and all previous models include the following. First, the model described in this report introduces the combined effects of film effectiveness and heat transfer augmentation due to film cooling. Secondly, no isothermal wall assumption is required. Finally, it is not necessary to measure the film effectiveness in a separate experiment with an adiabatic wall boundary condition. In other words, all of the test articles can have a realistic thermal conductivity.

Similar to all previous models, the current model is limited by a one-dimensional heat flow assumption. Another limitation of the current model is the lack of explicit terms that affect the film cooling performance such as blowing ratio, density ratio, etc. These limitations are also true of the previous models described above.

The overall goal for this effort is to demonstrate an alternative approach to estimate film effectiveness and heat transfer augmentation using local overall cooling effectiveness, or non-dimensional wall temperature, measurements. Conversely, if representative values for heat transfer without film cooling, h_0, heat transfer augmentation, h_f/h_0, and film effectiveness, η_f, are known, then it may be possible to predict the local wall temperature variations, or overall cooling effectiveness using this model.

2. MODEL DESCRIPTION

The model described in this paper is based on a simplified one-dimensional thermal resistance network illustrated in Figure 1. The heat flows from the hot gas stream through a plane wall and into a coolant stream. A fraction of the coolant inlet mass flow is extracted for film cooling, $\dot{m}_f$, and the remainder of the coolant channel inlet flow exits from the downstream edge for the area of interest. The cold side reference temperature for the resistance network, $T_{c,x}$, is an arbitrary temperature that is bounded by the coolant channel inlet and outlet temperatures, $T_{c,in}$ and $T_{c,out}$, respectively. The film temperature, T_f, is modeled as a weighted average between the free-stream hot gas temperature, T_g, and the film coolant exit temperature, $T_{c,e}$ (see Equation 9). This definition is consistent with the conventional definition of adiabatic film effectiveness.

$$T_f = \eta_f T_{c,e} + (1 - \eta_f) T_g \tag{9}$$

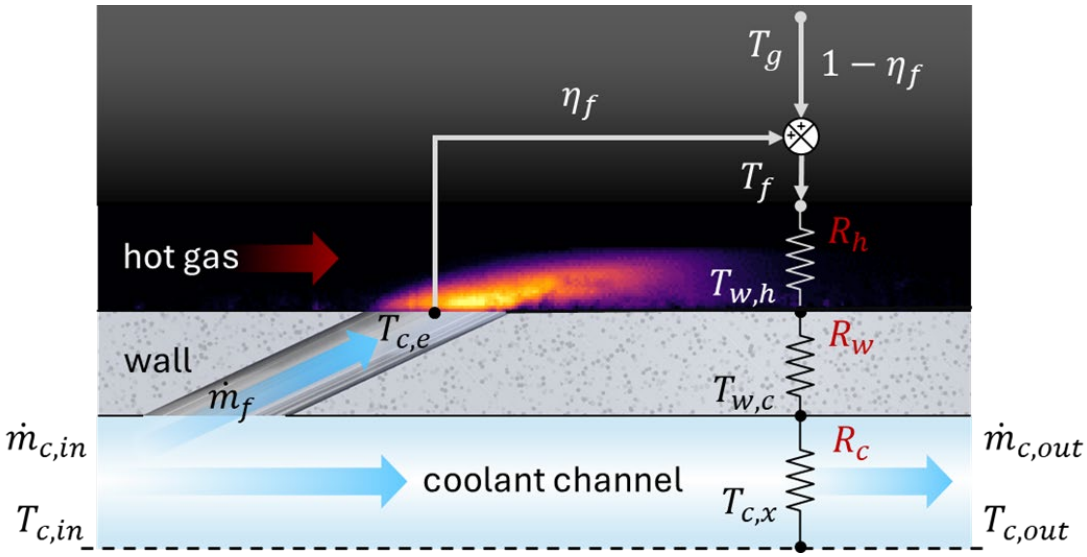

Figure 1: Simplified thermal resistance network for film cooling

Although the model described in Figure 1 was developed for a different purpose,[15] this model can also be used to describe local cooling effectiveness *with* and *without* film cooling. To represent the no film cooling case, two conditions are needed. First, if the film effectiveness is zero, ($\eta_f = 0$), then the driving temperature for the heat flux should be the freestream gas temperature, T_g. From Equation 9, this first condition is included in the model (i.e., $T_f = T_g$ when $\eta_f = 0$). Secondly, if there is no film cooling, then no heat transfer augmentation should occur (i.e., $\frac{h_f}{h_0} = 1$) and the subsequent thermal resistance should reflect the thermal resistance *without* film cooling, $R_{h,0}$. By applying these conditions to the resistance network model in Figure 1, the values predicted by the model are consistent with expectations for the baseline configuration *without* film cooling. In the following paragraphs, an analytical relationship will be derived to relate local surface temperature measurements, $T_{w,h}$, and film cooling performance metrics (i.e, η_f and $\frac{h_f}{h_0}$).

3. DERIVATION OF KEY RELATIONS

The purpose of this section is to document the steps and assumptions required to develop relationships between temperature differences and film cooling performance metrics. These details are documented here to inform in future studies and applications for the simple engineering model proposed in Figure 1.

3.1 LOCAL COOLING EFFECTIVENESS

Due to the one-dimensional assumption for the network shown in Figure 1, the heat flux through each segment of the network is constant. So, Equation 10 can be written directly to eliminate heat flux terms. Note that the cold reference temperature is a local coolant temperature, $T_{c,x}$, instead of the coolant inlet temperature. As a result, the expression derived in this section is not exactly the overall cooling effectiveness described by Equation 2. The corrections required to account for the deviations between $T_{c,x}$ and $T_{c,in}$ will be discussed in the next section.

$$\frac{T_{w,h} - T_{c,x}}{R_w + R_c} = \frac{T_f - T_{c,x}}{\left({h_{h,0}}/{h_f}\right) R_{h,0} + R_w + R_c} \tag{10}$$

Substituting the expression for film temperature from Equation 9 into 10.

$$\frac{T_{w,h} - T_{c,x}}{R_w + R_c} = \frac{\left[\eta_f T_{c,e} + (1-\eta_f) T_g\right] - T_{c,x}}{\left({h_{h,0}}/{h_f}\right) R_{h,0} + R_w + R_c} \tag{11}$$

By adding (and subtracting) $\eta_f T_{c,x}$ to the numerator, the expression can be split into two terms.

$$\frac{T_{w,h} - T_{c,x}}{R_w + R_c} = \frac{\eta_f T_{c,e} + (1-\eta_f) T_g - T_{c,x} + \eta_f T_{c,x} - \eta_f T_{c,x}}{\left({h_{h,0}}/{h_f}\right) R_{h,0} + R_w + R_c} \tag{12}$$

$$\frac{T_{w,h} - T_{c,x}}{R_w + R_c} = \frac{(1-\eta_f)(T_g - T_{c,x}) + \eta_f (T_{c,e} - T_{c,x})}{\left({h_{h,0}}/{h_f}\right) R_{h,0} + R_w + R_c} \tag{13}$$

$$\frac{T_{w,h} - T_{c,x}}{R_w + R_c} = \frac{(1-\eta_f)(T_g - T_{c,x})}{\left({h_{h,0}}/{h_f}\right) R_{h,0} + R_w + R_c} + \frac{\eta_f (T_{c,e} - T_{c,x})}{\left({h_{h,0}}/{h_f}\right) R_{h,0} + R_w + R_c} \tag{14}$$

Multiplying by $\frac{R_w + R_c}{(T_g - T_{c,x})}$

$$\frac{T_{w,h}-T_{c,x}}{T_g-T_{c,x}}=\frac{(1-\eta_f)(R_w+R_c)}{\left(h_{h,0}/h_f\right)R_{h,0}+R_w+R_c}+\frac{\eta_f(R_w+R_c)}{\left(h_{h,0}/h_f\right)R_{h,0}+R_w+R_c}\left[\frac{T_{c,e}-T_{c,x}}{T_g-T_{c,x}}\right] \tag{15}$$

For the case *without* film cooling (i.e., $\eta_f = 0$ and $\frac{h_f}{h_0} = 1$), the second term in Equation 15 becomes zero and the first term reduces to the expected ratio of thermal resistances.

If the thermal resistances are normalized by the (no-film) thermal resistance on the hot side, the key parameters of heat transfer augmentation, ($\frac{h_f}{h_0}$), and film effectiveness, η_f, become explicit terms as shown in Equation 16. For a plane wall, or flat plate, the heat transfer area in the thermal resistance terms will cancel, so the specific thermal resistance values can be used.

$$\frac{T_{w,h}-T_{c,x}}{T_g-T_{c,x}}=\frac{\frac{h_f}{h_0}(1-\eta_f)\left(\frac{R''_w}{R''_{h,0}}+\frac{R''_c}{R''_{h,0}}\right)}{1+\frac{h_f}{h_0}\left(\frac{R''_w}{R''_{h,0}}+\frac{R''_c}{R''_{h,0}}\right)}+\frac{\frac{h_f}{h_0}\eta_f\left(\frac{R''_w}{R''_{h,0}}+\frac{R''_c}{R''_{h,0}}\right)}{1+\frac{h_f}{h_0}\left(\frac{R''_w}{R''_{h,0}}+\frac{R''_c}{R''_{h,0}}\right)}\left[\frac{T_{c,e}-T_{c,x}}{T_g-T_{c,x}}\right] \tag{16}$$

3.2 CORRECTION FOR COOLANT WARMING EFFECT

Equation 16 is a key expression, but the cold side reference temperature, $T_{c,x}$, is different from the reference temperature, $T_{c,in}$, in the definition of the overall cooling effectiveness, ϕ (see Equation 2). The following paragraphs will focus on estimating a correction factor that relates the term, $T_g - T_{c,x}$, in Equation 16 to the denominator in the cooling effectiveness definition ($T_g - T_{c,in}$).

To define the coolant reference temperature, $T_{c,x}$, in terms of the inlet and outlet coolant temperature, a coolant warming factor, χ, is introduced. Although this warming factor is similar to the factor described in Williams et al.,[13] the definition in Equation 17 is different from prior work.[13]

$$T_{c,x} = (1-\chi)T_{c,in} + \chi T_{c,out} \tag{17}$$

If the heat transferred through the wall is absorbed by the coolant, then the following equation represents the energy balance.

$$\dot{m}_{out}c_pT_{c,out} - \dot{m}_{in}c_pT_{c,in} = \iint \frac{T_f - T_{c,x}}{\left(h_{h,0}/h_f\right)R_{h,0}+R_w+R_c}\,dz\,dx \tag{18}$$

The following assumptions are relevant to the remainder of this section:

1) The heat transfer area is the same for all thermal resistance terms, because a plane wall geometry is being assumed.
2) The mass flow rate used in Equation 18 represents the mass flow rate which shares a common wall with the area of interest. To illustrate difference between the mass flow rate used in Equation 18 and the mass flow rate of the coolant channel, consider the example shown in Figure 2. Although the derivation of this expression assumes a co-flow configuration, Figure 2 illustrates a crossflow configuration which is relevant for later sections in this report. The area of interest is denoted as a blue box in Figure 2. Although the coolant mass flux at the upstream edge of the area of interest is constant, the mass flow rate used in Equation 18 differs from the mass flow rate in the coolant channel. This relationship is summarized in Figure 2. This definition is important in the definition of heat load parameter that will be described later.
3) For completeness, this derivation will assume a co-linear flow configuration in which the mass flow along the downstream edge of the area of interest is smaller than the mass flow along the upstream edge of the area of interest. In summary, assume $\dot{m}_{out} = \dot{m}_{in} - \dot{m}_f$.

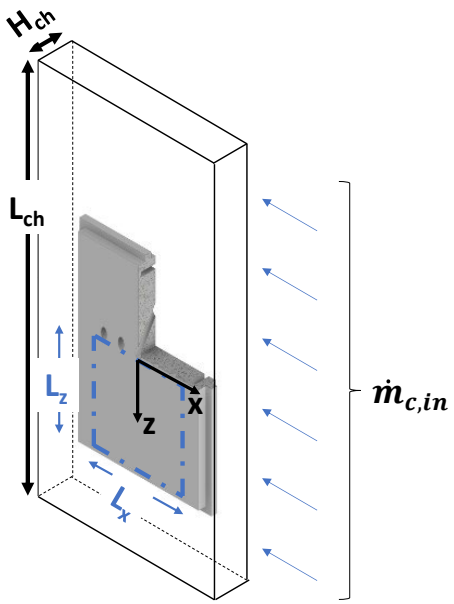

$$\frac{\dot{m}_{in}}{L_z H_{ch}} = \frac{\dot{m}_{c,in}}{L_{ch} H_{ch}}$$

$$\dot{m}_{in} = \frac{L_z}{L_{ch}} \dot{m}_{c,in}$$

Figure 2: Schematic relating the coolant channel inlet mass flow rate to the mass flow rate adjacent to the area of interest.

Substitute Assumption 3 into Equation 18,

$$\dot{m}_{in} c_p \left(T_{c,out} - T_{c,in}\right) - \dot{m}_f c_p T_{c,out} = \iint \frac{T_f - T_{c,x}}{\left(h_{h,0}/h_f\right) R_{h,0} + R_w + R_c} dz\, dx \tag{19}$$

The temperature at the outlet of the channel, $T_{c,out}$, can also be eliminated from the previous equation by solving for $T_{c,out}$, in Equation 17 and substituting into Equation 19.

$$\dot{m}_{in} c_p \left(\left[\frac{T_{c,x} - (1-\chi) T_{c,in}}{\chi} \right] - T_{c,in} \right) - \dot{m}_f c_p \left[\frac{T_{c,x} - (1-\chi) T_{c,in}}{\chi} \right] = \iint \frac{T_f - T_{c,x}}{\left(h_{h,0}/h_f\right) R_{h,0} + R_w + R_c} dz\, dx \tag{20}$$

Multiply by χ.

$$\dot{m}_{in}c_p\left(T_{c,x} - (1-\chi)T_{c,in} - \chi T_{c,in}\right) - \dot{m}_f c_p\left(T_{c,x} - (1-\chi)T_{c,in}\right) = \iint \frac{\chi(T_f - T_{c,x})}{\left({}^{h_{h,0}}/_{h_f}\right)R_{h,0} + R_w + R_c}\,dz\,dx \tag{21}$$

$$\dot{m}_{in}c_p\left(T_{c,x} - T_{c,in}\right) = \iint \frac{\chi(T_f - T_{c,x})}{\left({}^{h_{h,0}}/_{h_f}\right)R_{h,0} + R_w + R_c}\,dz\,dx + \dot{m}_f c_p\left(T_{c,x} - (1-\chi)T_{c,in}\right) \tag{22}$$

Substitute Equation 9 for T_f.

$$\dot{m}_{in}c_p\left(T_{c,x} - T_{c,in}\right) = \iint \frac{\chi\left(\left[\eta_f T_{c,e} + (1-\eta_f)T_g\right] - T_{c,x}\right)}{\left({}^{h_{h,0}}/_{h_f}\right)R_{h,0} + R_w + R_c}\,dz\,dx + \dot{m}_f c_p\left(T_{c,x} - (1-\chi)T_{c,in}\right) \tag{23}$$

Rearrange terms in the numerator of the integrand.

$$\dot{m}_{in}c_p\left(T_{c,x} - T_{c,in}\right) = \iint \frac{\chi\left[\left(T_g - T_{c,x}\right) + \eta_f\left(T_{c,e} - T_g\right)\right]}{\left({}^{h_{h,0}}/_{h_f}\right)R_{h,0} + R_w + R_c}\,dz\,dx + \dot{m}_f c_p\left(T_{c,x} - (1-\chi)T_{c,in}\right) \tag{24}$$

Use the following relation for the term on the left-hand side of the previous equation.

$$\left(T_{c,x} - T_{c,in}\right) = \left(T_g - T_{c,in}\right) - \left(T_g - T_{c,x}\right) \tag{25}$$

$$\dot{m}_{in}c_p\left(\left(T_g - T_{c,in}\right) - \left(T_g - T_{c,x}\right)\right) = \iint \frac{\chi\left[\left(T_g - T_{c,x}\right) + \eta_f\left(T_{c,e} - T_g\right)\right]}{\left({}^{h_{h,0}}/_{h_f}\right)R_{h,0} + R_w + R_c}\,dz\,dx + \dot{m}_f c_p\left(T_{c,x} - (1-\chi)T_{c,in}\right) \tag{26}$$

Divide by $\dot{m}_{in}c_p\left(T_g - T_{c,in}\right)$ and move the temperatures outside the integral.

$$1-\frac{T_g-T_{c,x}}{T_g-T_{c,in}}=\frac{T_g-T_{c,x}}{T_g-T_{c,in}}\left(\frac{1}{\dot{m}_{in}c_p}\right)\iint\frac{\chi}{\left({}^{h_{h,0}}\!/_{h_f}\right)R_{h,0}+R_w+R_c}\,dz\,dx+\frac{T_{c,e}-T_g}{T_g-T_{c,in}}\left(\frac{1}{\dot{m}_{in}c_p}\right)\iint\frac{\chi\,\eta_f}{\left({}^{h_{h,0}}\!/_{h_f}\right)R_{h,0}+R_w+R_c}\,dz\,dx+\frac{\dot{m}_f}{\dot{m}_{in}}\left(\frac{T_{c,x}-(1-\chi)T_{c,in}}{T_g-T_{c,in}}\right) \tag{27}$$

Collect like terms.

$$\left(1+\left(\frac{1}{\dot{m}_{in}c_p}\right)\iint\frac{\chi}{\left({}^{h_{h,0}}\!/_{h_f}\right)R_{h,0}+R_w+R_c}\,dz\,dx\right)\frac{T_g-T_{c,x}}{T_g-T_{c,in}}=1-\frac{T_{c,e}-T_g}{T_g-T_{c,in}}\left(\frac{1}{\dot{m}_{in}c_p}\right)\iint\frac{\chi\,\eta_f}{\left({}^{h_{h,0}}\!/_{h_f}\right)R_{h,0}+R_w+R_c}\,dz\,dx+\frac{\dot{m}_f}{\dot{m}_{in}}\left(\frac{T_{c,x}-(1-\chi)T_{c,in}}{T_g-T_{c,in}}\right) \tag{28}$$

Normalize the numerator and the denominator in the integrand by the surface area for heat transfer, S_f, and the following area averaged quantities can be defined.

$$\iint_{z_{min},x_{min}}^{z_{max},x_{max}}\frac{\chi}{\left({}^{h_{h,0}}\!/_{h_f}\right)R_{h,0}+R_w+R_c}\,dz\,dx=\overline{\overline{\chi U_f}}S_f \tag{29}$$

$$\iint_{z_{min},x_{min}}^{z_{max},x_{max}}\frac{\chi\,\eta_f}{\left({}^{h_{h,0}}\!/_{h_f}\right)R_{h,0}+R_w+R_c}\,dz\,dx=\overline{\overline{\chi\,\eta_f U_f}}S_f \tag{30}$$

Substitute Equations 29 and 30 into Equation 28.

$$\left(1+\left(\frac{1}{\dot{m}_{in}c_p}\right)\overline{\overline{\chi U_f}}S_f\right)\frac{T_g-T_{c,x}}{T_g-T_{c,in}}=1-\frac{T_{c,e}-T_g}{T_g-T_{c,in}}\left(\frac{1}{\dot{m}_{in}c_p}\right)\overline{\overline{\chi\,\eta_f U_f}}S_f+\frac{\dot{m}_f}{\dot{m}_{in}}\left(\frac{T_{c,x}-(1-\chi)T_{c,in}}{T_g-T_{c,in}}\right) \tag{31}$$

The negative sign in the second term is changed by changing signs in the numerator of the temperature ratio.

$$\left(1+\frac{\overline{\overline{\chi U_f}}S_f}{\dot{m}_{in}c_p}\right)\frac{T_g-T_{c,x}}{T_g-T_{c,in}} = 1+\left(\frac{\overline{\overline{\chi\eta_f U_f}}S_f}{\dot{m}_{in}c_p}\right)\frac{T_g-T_{c,e}}{T_g-T_{c,in}}+\frac{\dot{m}_f}{\dot{m}_{in}}\left(\frac{T_{c,x}-(1-\chi)T_{c,in}}{T_g-T_{c,in}}\right) \tag{32}$$

$$\frac{T_g-T_{c,x}}{T_g-T_{c,in}} = \frac{1}{\left(1+\frac{\overline{\overline{\chi U_f}}S_f}{\dot{m}_{in}c_p}\right)}+\frac{\frac{\overline{\overline{\chi\eta_f U_f}}S_f}{\dot{m}_{c,in}c_p}}{\left(1+\frac{\overline{\overline{\chi U_f}}S_f}{\dot{m}_{in}c_p}\right)}\frac{T_g-T_{c,e}}{T_g-T_{c,in}} + \frac{\frac{\dot{m}_f}{\dot{m}_{c,in}}}{\left(1+\frac{\overline{\overline{\chi U_f}}S_f}{\dot{m}_{in}c_p}\right)}\left(\frac{T_{c,x}-(1-\chi)T_{c,in}}{T_g-T_{c,in}}\right) \tag{33}$$

Multiply by $\frac{\frac{\dot{m}_{in}c_p}{\overline{\overline{\chi U_f}}S_f}}{\frac{\dot{m}_{in}c_p}{\overline{\overline{\chi U_f}}S_f}}$.

$$\frac{T_g-T_{c,x}}{T_g-T_{c,in}} = \frac{\frac{\dot{m}_{in}c_p}{\overline{\overline{\chi U_f}}S_f}}{\left(\frac{\dot{m}_{in}c_p}{\overline{\overline{\chi U_f}}S_f}+1\right)}+\frac{\overline{\overline{\chi\eta_f}}}{\left(\frac{\dot{m}_{in}c_p}{\overline{\overline{\chi U_f}}S_f}+1\right)}\frac{T_g-T_{c,e}}{T_g-T_{c,in}} + \frac{\frac{\dot{m}_f}{\dot{m}_{in}}\left(\frac{\dot{m}_{in}c_p}{\overline{\overline{\chi U_f}}S_f}\right)}{\left(\frac{\dot{m}_{in}c_p}{\overline{\overline{\chi U_f}}S_f}+1\right)}\left(\frac{T_{c,x}-(1-\chi)T_{c,in}}{T_g-T_{c,in}}\right) \tag{34}$$

Two points should be noted about Equation 34. First, if the warming factor has a value of zero (i.e., $\chi = 0$), then $T_{c,x} = T_{c,in}$ (see Equation 17) and the left-hand side of Equation 34 should be one. Secondly, this expression was derived for a collinear flow of coolant in which the coolant channel flow at the outlet was the difference between the coolant channel flow at the inlet and the mass flow of film coolant ejected through the film cooling holes. For a crossflow configuration like the one shown in Figure 2, $\dot{m}_f = 0$.

The final expression for the correction factor that accounts for warming effects in the coolant is described by Equation 34. In order for Equation 16 to include these warming effects, Equation 16 should be multiplied by Equation 34. This will be described in more detail after an order of

magnitude analysis determines which of the terms on the right-hand side of Equations 16 and 34 are significant.

3.3 ORDER OF MAGNITUDE ANALYSIS OF TERMS

In this section, the magnitude of the individual terms for Equations 16 and 34 will be investigated using experimental conditions that have been reported by Straub et al.[16] In this experiment, $T_g = 650K$ and $T_{c,x} = 345K$. The coolant channel flow rate was varied such that the coolant channel Reynolds number (based on the hydraulic diameter of the coolant channel, $D_{c,h} = 12\ mm$) varied from 7,000 to 14,000. The film cooling mass flow was kept constant by controlling the backpressure while the coolant channel Reynolds number was varied. The hot gas free stream conditions were also kept constant. These test conditions are summarized in Table 1.

Table 1: Test condition values/ranges for order of magnitude analysis

Parameter	Min	Max	Source
Coolant channel inlet mass flow, $\dot{m}_{c,in}$, (kg/s)	0.009	0.019	Dataset from Figure 3
Film cooling mass flow, $\dot{m}_f$, (kg/s)	2.42E-03	2.46E-03	Dataset from Figure 3
Coolant specific heat, c_p, (J/kg K)	1000	1000	Average value
Heat transfer area, S_f, for region of interest (m^2)	2.86E-03	2.86E-03	Region of interest for dataset in Figure 3
Area-weighted average heat transfer coefficient, $\overline{\overline{\alpha_0 \beta_0}}$, (W/$m^2$ K)	266.6	266.6	Dataset from Figure 3
Area-weighted average film effectiveness, $\overline{\overline{\left(\frac{\beta_1}{\beta_0}\right)}}$,	0.16	0.16	Dataset from Figure 3
Area-weighted specific resistances, $\overline{\overline{R_w + R_c}}$, (m^2 K/W)	0.011	0.019	Dataset from Figure 3
Hot gas temperature (K)	649.2	650.5	Dataset from Figure 3
Coolant inlet temperature, $T_{c,in}$ (K)	339.7	340.9	Dataset from Figure 3
Coolant outlet temperature, $T_{c,out}$ (K)	349.1	350.1	Dataset from Figure 3
Warming factor, χ	0	1	Random normal distribution
Area-weighted average warming factor, $\bar{\bar{\chi}}$	0.5	0.5	Definition of χ
Film cooling hole exit temperature, $T_{c,e}$, (K)	$T_{c,in}$	$\overline{\overline{T_{w,h}}}$	Random normal distribution

3.3.1 -- Order of magnitude analysis for Equation 16

Equation 16 is rewritten in terms of regression coefficients described below. In Straub et al.,[16] the α_0 regression coefficient is found from a training dataset *without* film cooling. Similarly, the β_0 and β_1 regression coefficients are found from a training dataset *with* film cooling. These

regression coefficients are spatially dependent, so the regression is performed at each pixel in the IR temperature measurements for $T_{w,h}$. Additional details on the approach to find these model regression coefficients are provided in Straub et al.[16]

$$\frac{T_{w,h}-T_{c,x}}{T_g-T_{c,x}}=\frac{\alpha_0(\beta_0-\beta_1)(R''_w+R''_c)}{1+\alpha_0\beta_0(R''_w+R''_c)}+\frac{\alpha_0\beta_1(R''_w+R''_c)}{1+\alpha_0\beta_0(R''_w+R''_c)}\left[\frac{T_{c,e}-T_{c,x}}{T_g-T_{c,x}}\right]$$
$$\frac{T_{w,h}-T_{c,x}}{T_g-T_{c,x}}= \quad \boldsymbol{Eq16-Term\,1} \quad + \quad \boldsymbol{Eq16-Term\,2} \tag{35}$$

$$\alpha_0=\frac{1}{\widehat{R''_{h,0}}}=\widehat{h_0}$$
$$\beta_0=\widehat{\left(\frac{h_f}{h_0}\right)} \tag{36}$$
$$\beta_1=\widehat{\frac{h_f}{h_0}\eta_f}$$

The objective of this section is to investigate the relative magnitude of the terms on the right-hand side of Equation 16 (see also Eq. 35). The training datasets *with* film cooling will be used to make these comparisons. The measured wall temperatures for these datasets are shown in Figure 3a. In Figure 3, the hot gas flow direction is from top-to-bottom and the coolant supply flow direction is from right-to-left. The specific thermal resistances for the coolant side, R''_c, and the wall, R''_w, are calculated using the expressions shown in Equation 37 and 38, respectively. These specific thermal resistance values are shown in Figure 3b and Figure 3c. In Equation 38, the thermal conductivity of the solid, k_w, is treated as a temperature dependent property using the temperature measured in Figure 3a. For each coolant channel Reynolds number shown in Figure 3, there are approximately 132,000 datapoints.

$$R''_c=\frac{1}{h_c}=\frac{1}{\left(\frac{k_c}{D_h}\right)0.023Re_c^{0.8}Pr^{0.33}} \tag{37}$$

$$R''_w=\frac{t}{k_w} \tag{38}$$

Using the datasets in Figure 3, the relative magnitude of the terms on the right-hand side of Equation 35 will be assessed. For Term 1, all parameters are known.

For Term 2, the temperature at the exit of the film cooling hole, $T_{c,e}$, is not known. However, this temperature can be bounded between the coolant inlet temperature, $T_{c,in}$, and the wall temperature, $T_{w,h}$. By treating $T_{c,e}$ as a random variable with a mean that is midway between the limits and a standard deviation that is 1/6 of the variance between the limits, a statistical approximation can be estimated. Using this approach, Figure 4 shows that Term 2 is significantly smaller than the values for Term 1. In an attempt to quantify the differences, the cumulative distribution function (i.e., bottom panel in Figure 3) shows that roughly 95% of the Term 2

values are less than ten percent of Term 1 values. Based on this analysis, the second term is an order of magnitude smaller than Term 1, so neglecting the second term in Equation 16 will have a small (less than 10 percent) effect.

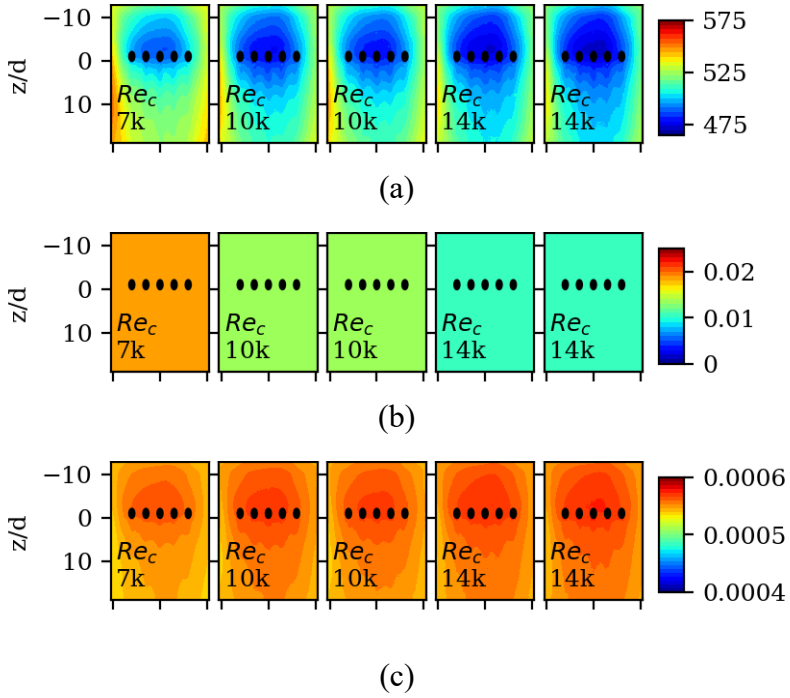

Figure 3: Sample datasets used as an example. a) Experimentally measured wall temperatures [K] as function of coolant channel Reynold's number; b) Specific thermal resistance [m^2 K/W] on cold side of wall (Eq. 37); c) Specific thermal resistance [m^2 K/W] for conduction through a plane wall (Eq. 38).

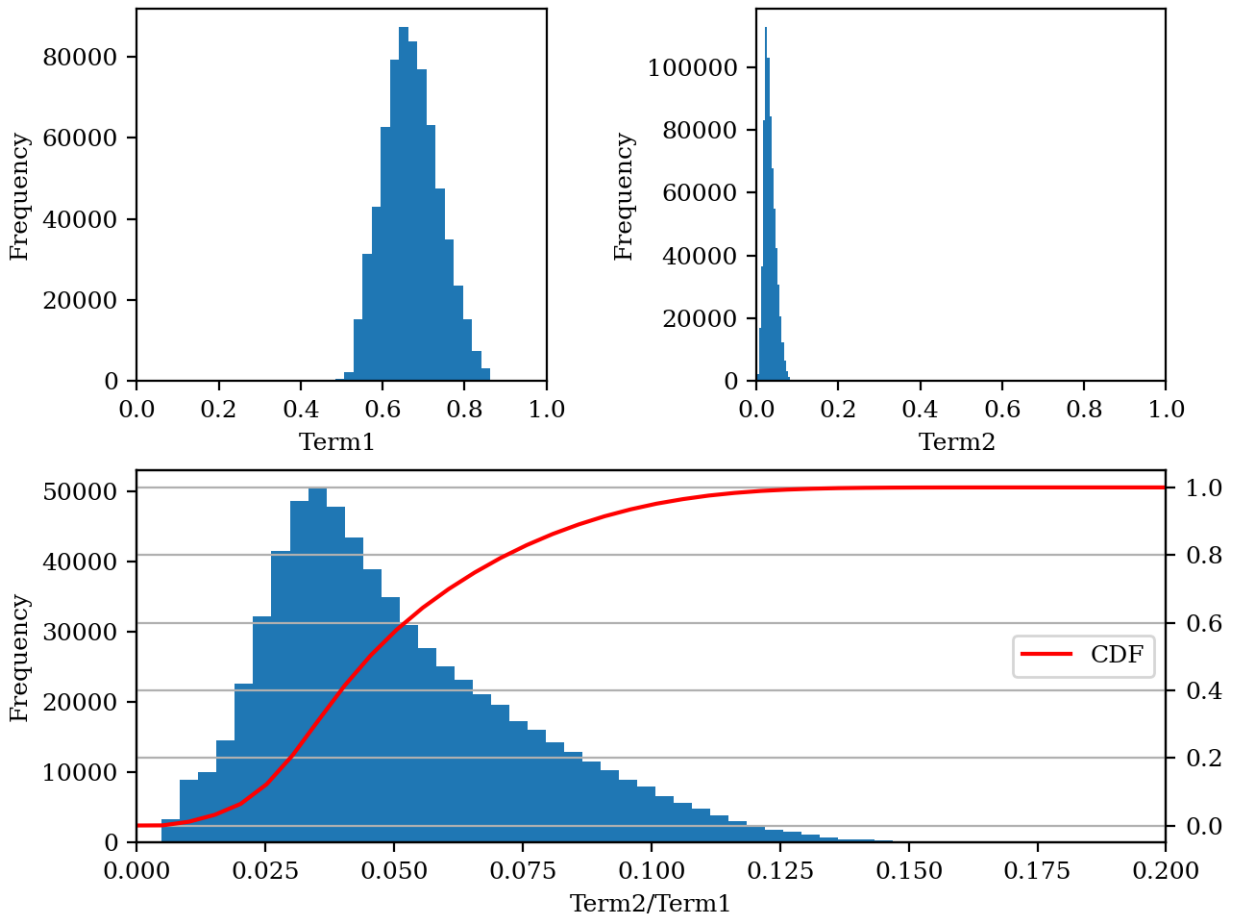

Figure 4: Histograms from example dataset comparing the relative magnitude of terms in Equation 35

3.3.2 – Order of magnitude analysis for Equation 34

The relative magnitude of terms derived for the coolant warming correction factor (see Section 3.2) will be investigated in this section. Equation 34 is re-written below in terms of a heat load parameter, W_f^+.

$$\frac{T_g - T_{c,x}}{T_g - T_{c,in}} = \frac{W_f^+/\bar{\bar{\chi}}}{\left(W_f^+/\bar{\bar{\chi}} + 1\right)} + \frac{\bar{\bar{\chi}}\overline{\overline{\left(\beta_1/\beta_0\right)}}}{\left(W_f^+/\bar{\bar{\chi}} + 1\right)}\frac{T_g - T_{c,e}}{T_g - T_{c,in}} + \frac{\dot{m}_f}{\dot{m}_{c,in}}\frac{\left(W_f^+/\bar{\bar{\chi}}\right)}{\left(W_f^+/\bar{\bar{\chi}} + 1\right)}\left(\frac{\chi T_{c,out}}{T_g - T_{c,in}}\right) \tag{39}$$

$$W_f^+ = \frac{\dot{m}_{in}c_p}{\overline{\overline{U_f}}S_f} = \frac{\dot{m}_{in}c_p}{S_f}\left[\overline{\overline{\left(h_{h,0}/h_f\right)R''_{h,0} + R''_w + R''_c}}\right] \tag{40}$$

$$W_f^+ = \frac{\dot{m}_{in} c_p}{S_f} \left[\overline{\overline{\frac{1}{\alpha_0 \beta_0} + R_w'' + R_c''}} \right] = \frac{\overline{\overline{T_f - T_{c,x}}}}{T_{c,out} - T_{c,in}} \tag{41}$$

In the derivation of the heat load parameter term (see Section 3.2), the coolant mass flow rate and the heat transfer area were defined with respect to a common wall. For the parameters listed in Table 1 the heat transfer area, S_f, represents the surface area downstream of the film cooling holes. This region of interest is shown schematically in Figure 5 as a dashed blue box. Compared to the cross-sectional flow area of the entire coolant channel, the heat load parameter needs to be redefined. In other words, since the transverse dimension for the region of interest differs from the transverse dimension of the channel, the relative mass flowrate in the heat load parameter should be modified as summarized in Figure 5.

The terms from the right-hand side of Equation 34 will be re-written below. Using the training dataset summarized in Figure 3 and Table 1, the magnitude of Term 1 ranges between 0.986 and 0.990.

$$\boldsymbol{Eq34 - Term\ 1} = \frac{W_f^+}{\left(W_f^+ + \bar{\bar{\chi}}\right)} \approx 0.99 \tag{42}$$

$$\boldsymbol{Eq34 - Term\ 2} = \frac{\bar{\bar{\chi}} \overline{\overline{\left(\frac{\beta_1}{\beta_0}\right)}}}{\left(\frac{W_f^+}{\bar{\bar{\chi}}} + 1\right)} \frac{T_g - T_{c,e}}{T_g - T_{c,in}} \approx 0.001 \tag{43}$$

$$\boldsymbol{Eq34 - Term\ 3} = \frac{\frac{\dot{m}_f}{\dot{m}_{in}}\left(W_f^+\right)}{\left(W_f^+ + \bar{\bar{\chi}}\right)} \left(\frac{\chi T_{c,out}}{T_g - T_{c,in}} \right) \tag{44}$$

Term 2 is approximately three orders of magnitude smaller than Term 1, so this term can be neglected without significant error.

Term 3 can be significant depending on the ratio of the film coolant mass flow that is extracted from the inlet coolant flowrate. Although the derivation of this expression assumed a co-flow configuration, for the example datasets, the coolant was fed by a perpendicular crossflow as shown in Figure 5. For the region of interest denoted in Figure 5, the mass flow into the region of interest is the same as the outlet, so Term 3 should be zero. Therefore, for the crossflow configuration and region of interest identified in this example, only the first term on the right-hand side of Equation 34 is significant, and this term is very close to 1.0

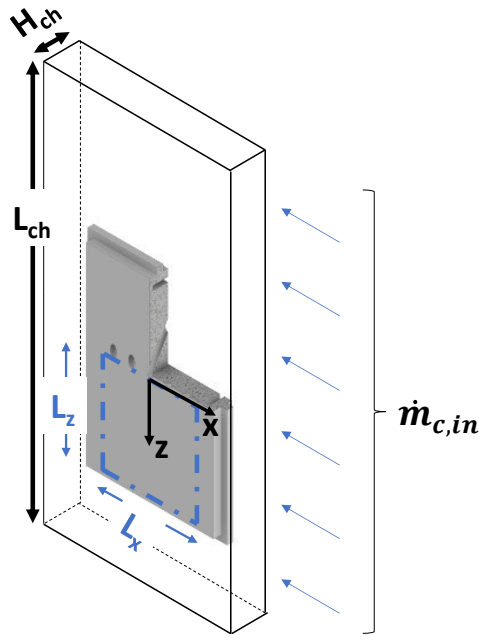

$$\dot{m}_{in} = \frac{\dot{m}_{c,in}(L_z H_{ch})}{L_{ch} H_{ch}} = \frac{L_z}{L_{ch}} \dot{m}_{c,in}$$

$$S_f = L_z L_x$$

$$\frac{\dot{m}_{in} c_p}{S_f} = \frac{L_z}{L_{ch}} \dot{m}_{c,in} \cdot \frac{c_p}{L_z L_x}$$

$$\frac{\dot{m}_{in} c_p}{S_f} = \frac{\dot{m}_{c,in} c_p}{L_{ch} L_x}$$

$$W_f^+ = \frac{\dot{m}_{c,in} c_p}{L_{ch} L_x} \left[\frac{1}{\alpha_0 \beta_0} + R_w'' + R_c'' \right]$$

Figure 5: Schematic relating the coolant channel inlet mass flow rate to the mass flow rate in the definition of heat load parameter.

3.4 OVERALL COOLING EFFECTIVENESS RELATIONS

Using the information from the previous sections, the relationship between overall cooling effectiveness, film effectiveness, and heat transfer augmentation due to film cooling can be written by combining the most significant terms from Equations 16 and 34. First, the following relationship is used to simplify the left-hand side of Equation 16.

$$T_{w,h} - T_{c,x} = T_{w,h} - T_{c,x} + T_g - T_g = (T_g - T_{c,x}) - (T_g - T_{w,h}) \tag{45}$$

$$\frac{T_{w,h} - T_{c,x}}{T_g - T_{c,x}} = \frac{(T_g - T_{c,x}) - (T_g - T_{w,h})}{T_g - T_{c,x}} \tag{46}$$

Rewrite Equation 16 but neglect the second term on the right-hand side. The second term is neglected based on the order of magnitude analysis described in the previous section.

$$1 - \frac{T_g - T_{w,h}}{T_g - T_{c,x}} = \frac{(1 - \eta_f)(R_w'' + R_c'')}{\left({}^{h_{h,0}}/_{h_f} \right) R_{h,0}'' + R_w'' + R_c''} \tag{47}$$

Solve for $\frac{T_g - T_{w,h}}{T_g - T_{c,x}}$.

$$\frac{T_g - T_{w,h}}{T_g - T_{c,x}} = 1 - \frac{\left(1-\eta_f\right)\left(R''_w + R''_c\right)}{\left({}^{h_{h,0}}\!/_{h_f}\right) R''_{h,0} + R''_w + R''_c} \tag{48}$$

Incorporate the correction factor for the coolant warming effects. Although Term 3 is not significant in the example dataset, Term 3 will be included in the derivation for completeness.

$$\frac{T_g - T_{w,h}}{T_g - T_{c,x}} \cdot \frac{T_g - T_{c,x}}{T_g - T_{c,in}} = \left[1 - \frac{\left(1-\eta_f\right)\left(R''_w + R''_c\right)}{\left({}^{h_{h,0}}\!/_{h_f}\right) R''_{h,0} + R''_w + R''_c}\right] \cdot \frac{W_f^+}{W_f^+ + \bar{\bar{\chi}}}\left[1 + \frac{\dot{m}_f}{\dot{m}_{in}}\left(\frac{\chi T_{c,out}}{T_g - T_{c,in}}\right)\right] \tag{49}$$

Using the definition of overall cooling effectiveness, $\phi = \frac{T_g - T_{w,h}}{T_g - T_{c,in}}$, the previous equation can be reduced to the following.

$$\phi_f = \left[1 - \frac{\left(1-\eta_f\right)\left(R''_w + R''_c\right)}{\left({}^{h_{h,0}}\!/_{h_f}\right) R''_{h,0} + R''_w + R''_c}\right] \cdot \frac{W_f^+}{W_f^+ + \bar{\bar{\chi}}}\left[1 + \frac{\dot{m}_f}{\dot{m}_{in}}\left(\frac{\chi T_{c,out}}{T_g - T_{c,in}}\right)\right] \tag{50}$$

Isolate the variable, $(R_w + R_c)$, and multiply numerator and denominator by $\frac{h_f}{h_{h,0}}\frac{1}{R_{h,0}}$.

$$\phi_f = \left[1 - \frac{\frac{h_f}{h_{h,0}}\left(1-\eta_f\right)\frac{1}{R''_{h,0}}\left(R''_w + R''_c\right)}{1 + \left(\frac{h_f}{h_{h,0}}\right)\frac{1}{R''_{h,0}}\left(R''_w + R''_c\right)}\right] \cdot \frac{W_f^+}{W_f^+ + \bar{\bar{\chi}}}\left[1 + \frac{\dot{m}_f}{\dot{m}_{c,in}}\left(\frac{\chi T_{c,out}}{T_g - T_{c,in}}\right)\right] \tag{51}$$

$$W_f^+ = \frac{\dot{m}_{in} c_p}{\overline{\overline{U_f}} S_f} = \frac{\dot{m}_{in} c_p}{S_f}\left[\overline{\left({}^{h_{h,0}}\!/_{h_f}\right) R''_{h,0} + R''_w + R''_c}\right] \tag{52}$$

Note that this equation can also be used to describe the overall cooling effectiveness for a case without film cooling, by setting $\eta_f = 0$, $\dot{m}_f = 0$, and $\frac{h_f}{h_0} = 1$.

$$\phi_0 = \left[1 - \frac{\frac{1}{R''_{h,0}}(R''_w + R''_c)}{1 + \frac{1}{R''_{h,0}}(R''_w + R''_c)}\right] \cdot \frac{W_0^+}{(W_0^+ + \bar{\bar{\chi}})} \tag{53}$$

$$W_0^+ = \frac{\dot{m}_{in} c_p}{\overline{\overline{U_0}} S_0} = \frac{\dot{m}_{in} c_p}{S_0} \overline{\overline{\left[R''_{h,0} + R''_w + R''_c\right]}} = \frac{\dot{m}_{in} c_p}{S_0} \overline{\overline{\left[\frac{1}{\alpha_0} + R''_w + R''_c\right]}} \tag{54}$$

3.5 DISCUSSION OF MODEL COOLING EFFECTIVENESS RELATIONS

The equations derived in the previous section will be discussed in this section with particular emphasis on the predicted trends from these model relations. In Section 3.3.2, the values for W_f^+ were in the range of $36 < W_f^+ < 48$ using a heat transfer area shown schematically in Figure 4 (i.e., $-7.5\text{d} < \text{x} < 7.5\text{d}$ and $0 < z < 19d$). The film cooling hole diameter, d, for the example dataset is 3.2mm.

Using the same region of interest, the heat load parameter *without* film cooling, W_0^+, can be calculated using Equation 54 and these W_0^+ values are similar to W_f^+ (i.e., $35 < W_0^+ < 45$). Similarly, for this example the values for the correction factor in Equation 53, (i.e., $\frac{W_0^+}{(W_0^+ + \bar{\bar{\chi}})}$) range from 0.986-0.990. In other words, this correction factor term, $\frac{W_0^+}{(W_0^+ + \bar{\bar{\chi}})}$, can be neglected.

So, Equation 53 can be simplified to the following.

$$\phi_0 = 1 - \frac{\frac{1}{R''_{h,0}}(R''_w + R''_c)}{1 + \frac{1}{R''_{h,0}}(R''_w + R''_c)} = 1 - \frac{\alpha_0(R''_w + R''_c)}{1 + \alpha_0(R''_w + R''_c)} \tag{55}$$

Let's consider the limits of this expression. If the specific thermal resistances R''_w and R''_c approach zero, the cooling effectiveness approaches 1 (i.e., $T_{w,h} \cong T_{c,in}$). If the sum of R''_w and R''_c become very large relative to $R''_{h,0}$, then the cooling effectiveness approaches zero (i.e., $T_{w,h} \cong T_g$). From a practical perspective, both limits seem unrealistic.

As an example, data from a flat plate experiment will be used to illustrate a modification to Equation 53. Area-averaged cooling effectiveness data for a flat plate *without* film cooling holes are shown as symbols in Figure 6. Two 'best-fit' regression lines are also shown. The dashed regression line (Equation 55) asymptotes to a value of zero as the specific thermal resistance becomes large. The solid 'best-fit' line (Equation 56) asymptotes to a value of $1 - \alpha_1 = 0.19$. From a practical perspective, this is the cooling effectiveness that would be approached if a very large thermal resistance on the cold side was present (i.e., no significant coolant flowing along

the cold surface). In other words, the temperature difference between the hot wall and the gas stream will asymptote to a non-zero value that may be dependent on the test apparatus. The wall temperature for a flat plate will never reach the free-stream hot gas temperature as Equation 53 suggests. Therefore, in order to get a better fit to the experimental data for the case without film cooling, Equation 55 is modified to include a correction factor, α_1, as shown in Equation 56.

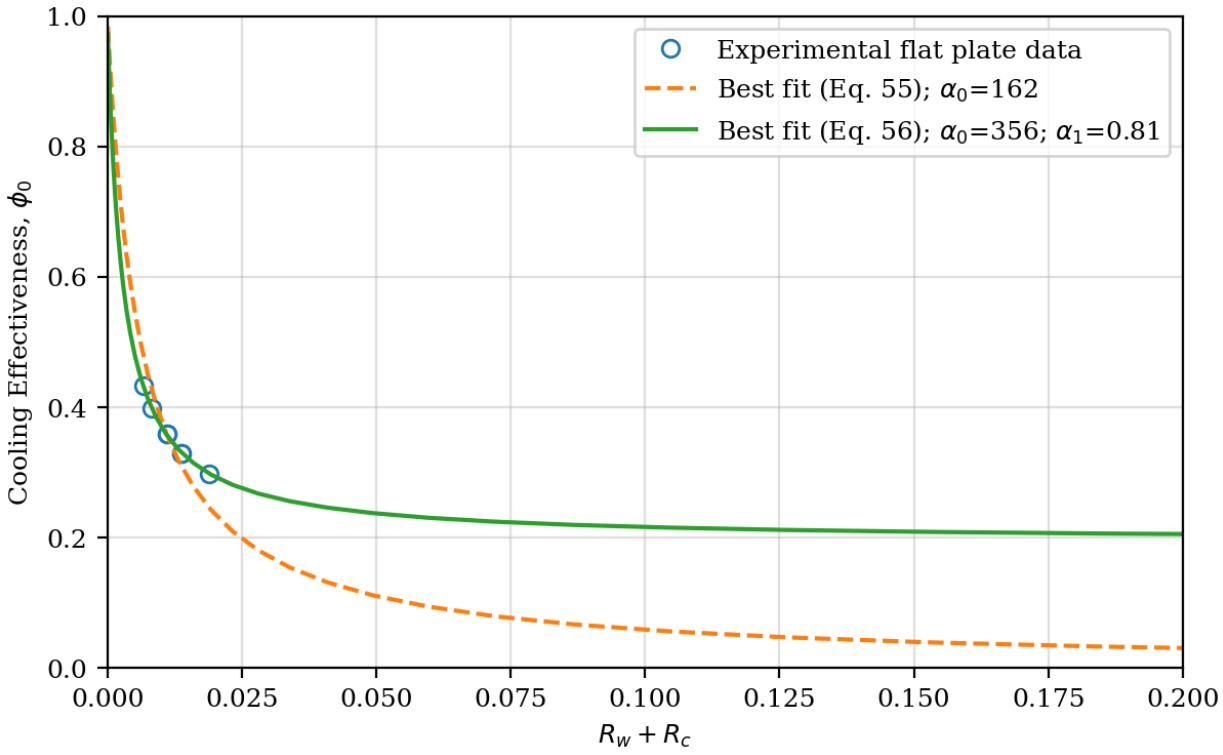

Figure 6: Cooling effectiveness as a function of specific cold side resistances for a flat plate without film cooling holes

$$\phi_0 = 1 - \alpha_1 \frac{\frac{1}{R''_{h,0}}(R''_w + R''_c)}{1 + \frac{1}{R''_{h,0}}(R''_w + R''_c)} = 1 - \alpha_1 \frac{\alpha_0(R''_w + R''_c)}{1 + \alpha_0(R''_w + R''_c)} \tag{56}$$

In summary, two key points have been discussed in this section. First, based on the experimental datasets considered in this report, the correction factors for the coolant warming effect (i.e., $\frac{w_0^+}{(w_0^+ + \bar{\bar{\chi}})}$ and $\frac{w_f^+}{(w_f^+ + \bar{\bar{\chi}})}$) were approximately 0.99 and considered negligible. It is important to carefully define the mass flow rate with respect to the heat transfer area as described in Figure 5.

Secondly, there is some discrepancy between the theoretical limits of cooling effectiveness predicted by the simplified model and the practical limits that may be test rig specific. When this model is used to fit experimental data from a cooling configuration *without* film cooling, a correction factor, α_1, provides a much better fit. This correction factor, α_1, represents a practical limit on the cooling effectiveness as the specific thermal resistance of cold side approaches infinity.

3.6 REGRESSION MODEL EQUATIONS

In this section, an approach to estimate key film cooling performance metrics will be described. By measuring local cooling effectiveness as a function of the coolant channel mass flow rate for 1) a configuration *without* film cooling, and 2) a configuration *with* film cooling these film cooling performance metrics can be estimated by curve-fitting two separate regression models to the experimental datasets.

The approach is based on the validity of the following assumptions:

- The specific thermal resistance on the coolant side (i.e., R_c'') is known or can be approximated using a correlation with coolant channel flowrate dependence. For example, the Dittus-Boelter correlation (see Equation 37).
- The specific thermal resistance for the wall (i.e., R_w'') can be approximated using the temperature measured on the hot surface and Equation 38.
- The coolant warming correction factor *with* and *without* film cooling is approximately one.
    - For example, $\frac{W_0^+}{(W_0^+ + \overline{\overline{\chi}})} \approx \frac{W_f^+}{(W_f^+ + \overline{\overline{\chi}})} \approx 1$, and
    - The total mass flowrate extracted for film cooling is approximately zero such that the following term, $\frac{\dot{m}_f}{\dot{m}_{in}}$, can be neglected (i.e., $\frac{\dot{m}_f}{\dot{m}_{in}}\left(\frac{\chi T_{c,out}}{T_g - T_{c,in}}\right) \approx 0$).
- If the film cooling flowrate, $\dot{m}_f$, can be controlled independent of the coolant channel supply flowrate, $\dot{m}_{c,in}$, then this approach assumes the film cooling performance metrics do not change as a result of changing the coolant channel mass flow rate. Lee et al. 2023 have shown that this assumption is more likely for low coolant channel mass flow rates and higher film cooling mass flows or blowing ratio conditions.

3.6.1 Cooling effectiveness *without* film cooling

As described in the previous section, the following model regression equation should relate overall cooling effectiveness to the sum of these two specific resistance terms.

$$\widehat{\phi_0} = 1 - \frac{\alpha_0(R_w'' + R_c'')}{1 + \alpha_0(R_w'' + R_c'')} \cdot \alpha_1 + \epsilon_0 \tag{57}$$

The regression coefficient, α_0, is an estimate of the hot side heat transfer coefficient without film cooling (see Equation 36). The regression coefficient, α_1, represents the practical limit for the test setup as mass flow rate of coolant in the coolant channel approaches zero. The error

discrepancy between the measured overall cooling effectiveness data and the model regression is represented by term, ϵ_0.

3.6.2 Cooling effectiveness *with* film cooling

The regression equation for the cooling effectiveness *with* film cooling is based on Equation 51 and the order of magnitude analysis that suggests the correction factor for the coolant warming can be neglected.

$$\widehat{\phi_f} = 1 - \frac{(\beta_0 - \beta_1)\alpha_0(R_w'' + R_c'')}{1 + \beta_0\alpha_0(R_w'' + R_c'')} \cdot \alpha_1 + \epsilon_f \tag{58}$$

In this expression, the regression coefficients, α_0 and α_1, are found from the regression of the datasets *without* film cooling. The regression coefficient, β_0, is an estimate of the heat transfer augmentation, h_f/h_0. The regression coefficient, β_1, is an estimate of the product of the heat transfer augmentation and the film effectiveness (i.e., $\beta_1 = \frac{h_f}{h_0}\eta_f$). Table 2 summarizes the regression coefficients and how they relate to key cooling performance metrics.

Table 2: Summary of regression coefficients and representative estimates for film cooling performance metrics

Regression Coefficient	Cooling Metric	Regression Equation	Data Source
$\boldsymbol{\alpha_0}$	$\widehat{h_0}$	Eq. 57	*Without* film cooling
$\boldsymbol{\alpha_1}$	$\lim_{R_c''\to\infty} \widehat{\phi_0}$	Eq 57	*Without* film cooling
$\boldsymbol{\beta_0}$	$\widehat{\frac{h_f}{h_0}}$	Eq. 58	*With* film cooling
$\boldsymbol{\beta_1}$	$\widehat{\frac{h_f}{h_0}\eta_f}$	Eq. 58	*With* film cooling

4. SUMMARY AND CONCLUSIONS

This report summarizes a simplified film cooling model that is based on a one-dimensional thermal resistance network previously reported by Searle et al.[15] In addition to the derivation details provided in this report, a coolant warming correction factor is also derived from a simplified heat balance between the coolant stream and the heat transfer area of interest. Experimental datasets from NETL's Conjugate Aerothermal Test rig are used to assess the magnitude of terms in the model equations, a key step in developing the model regression equations.

The model and experimental approach outlined in this report can be used to estimate local heat transfer coefficients, and adiabatic film effectiveness parameters in a non-adiabatic test rig. The approach uses hot side temperature measurements (with and without film cooling) at different coolant channel flow rates. Since heat flux values are not required, this approach is faster to implement than other approaches that required three-dimensional finite element modeling. Additionally, there is no need to make measurements using an adiabatic test article.

By curve fitting the experimental local overall cooling effectiveness (or normalized wall temperature) data to the regression model equations outlined in this report, estimates of the film effectiveness and the heat transfer augmentation due to film cooling can be found from the regression coefficients summarized in Table 2. The model and regression equations described in this report are a significant departure from previous models and preliminary data suggest that the model is capable of accurately predicting spatial variations in temperature as a function of coolant channel mass flow.

Future efforts should focus on validating the regression model equations discussed in this report in different geometries and test rigs. This approach has the potential to predict temperature variations upstream of the film cooling holes which cannot be estimated using current state-of-the-art cooling models. However, more data is needed to verify this potential.

5. REFERENCES

1. Bogard, D.G. (2006) "Airfoil Film Cooling," in *The Gas Turbine Handbook*, pp. 309–321. Available at: https://netl.doe.gov/carbon-management/turbines/handbook
2. Han, J.C., Dutta, S. and Ekkad, S. (2012) *Gas Turbine Heat Transfer and Cooling Technology*. 2nd Ed. Boca Raton: CRC Press. Available at: https://doi.org/10.1201/b13616
3. Shih, T.I.-P. and Yang, V. (2014) *Turbine aerodynamics, heat transfer, materials, and mechanics*. Edited by T. I-P. Shih and V. Yang. AIAA. Available at: https://doi.org/10.2514/4.102660
4. Forth, C.J.P. (1985) *An Investigation of Scaling Parameters Governing Film-Cooling*, Ph.D. Thesis, University of Oxford
5. Eriksen, V.L., Eckert, E.R.G. and Goldstein, R.J. (1971) *A Model for Analysis of the Temperature Field Downstream of a Heated Jet Injected Into an Isothermal Crossflow at an Angle of 90°*. Available at: https://ntrs.nasa.gov/citations/19720007294 (Accessed: January 7, 2025).
6. Holland, M.J. and Thake, T.F. (1980) "Rotor blade cooling in high pressure turbines," *Journal of Aircraft*, 17(6), pp. 412–418. Available at: https://doi.org/10.2514/3.44668
7. Young, J.B. and Wilcock, R.C. (2002) "Modeling the Air-Cooled Gas Turbine: Part 2—Coolant Flows and Losses," ASME. *J. Turbomach*, 124(2), p. 214. Available at: https://doi.org/10.1115/1.1415038
8. Torbidoni, L., and Horlock, J. H. (2005). "A New Method to Calculate the Coolant Requirements of a High-Temperature Gas Turbine Blade" ASME. *J. Turbomach.,* 127(1): 191–199. https://doi.org/10.1115/1.1811100
9. Downs, J.P. and Landis, K.K. (2009) "Turbine Cooling Systems Design: Past, Present and Future," *ASME Turbo Expo 2009, ASME GT2009-59991*, https://doi.org/10.1115/GT2009-59991
10. Straub, D. *et al.* (2022) *Advanced Airfoil Cooling Schemes to Increase Efficiency in Gas Turbines for Combined Heat and Power Applications*. Available at: https://netl.doe.gov/energy-analysis/search
11. Albert, J.E., Bogard, D.G. and Cunha, F. (2004) "Adiabatic and Overall Effectiveness for a Film Cooled Blade," in *ASME TurboExpo 2004*. ASME GT2004-53998, https://doi.org/10.1115/GT2004-53998
12. Albert, J.E. and Bogard, D.G. (2013) "Measurements of Adiabatic Film and Overall Cooling Effectiveness on a Turbine Vane Pressure Side with a Trench," *ASME. J. Turbomach.* 135(5), https://doi.org/10.1115/1.4007820
13. Williams, R.P. *et al.* (2013) "Sensitivity of the Overall Effectiveness to Film Cooling and Internal Cooling on a Turbine Vane Suction Side," A*SME. J. Turbomach.,* 136(3), https://doi.org/10.1115/1.4024681
14. Dyson, T.E. *et al.* (2013) "Adiabatic and overall effectiveness for a fully cooled turbine vane," in *ASME Turbo Expo 2013,* ASME GT2013-94928, https://doi.org/10.1115/GT2013-94928
15. Searle, M., Robey, E. and Straub, D. (2024) *A One-dimensional Heat Transfer Model for a Cooled Airfoil in a Direct-fired Supercritical CO_2 Turbine*. Available at: https://doi.org/10.2172/2377344
16. Straub, D., Tulgestke, A., Searle, M., Grabowski, W., and Weber, J. (2025) "Simplified model and approach to transform infrared surface temperatures to film effectiveness in

a conjugate heat transfer experiment," *submitted for publication in ASME TurboExpo 2025*. ASME GT2025-153214

U.S. DEPARTMENT of ENERGY

Marianne Walck
Director
National Energy Technology Laboratory
U.S. Department of Energy

John Wimer
Acting Chief Research Officer
Science & Technology Strategic Plans
& Programs
National Energy Technology Laboratory
U.S. Department of Energy

Bryan Morreale
Associate Laboratory Director for
Research & Innovation
Research & Innovation Center
National Energy Technology Laboratory
U.S. Department of Energy

NETL Technical Report Series